

Cardiac CT Prior to Left Atrial Appendage Closure Device Implantation and Percutaneous Mitral Valve Interventions

Swaminatha V. Gurudevan · Reza Arsanjani

Published online: 30 August 2014
© Springer Science+Business Media New York 2014

Abstract Recent advances in percutaneous techniques have allowed them to emerge as an attractive alternative to surgery in select patients. Left atrial appendage closure has emerged as a novel therapeutic option in patients with nonvalvular atrial fibrillation who cannot take anticoagulation therapy. Furthermore, percutaneous mitral valve procedures have shown promising results in high risk patients. These percutaneous procedures require multimodality imaging for preprocedural planning and during the procedure. Computed tomography has emerged as an attractive imaging modality prior to percutaneous procedures given its ability to perform comprehensive assessment of cardiac and extracardiac structures. This review assesses the role of computed tomography as it pertains to left atrial appendage occlusion and mitral valve transcatheter procedures.

Keywords Left atrial appendage · Structural heart intervention · Percutaneous mitral valve repair · Cardiac computed tomography

Introduction

Advances in transcatheter techniques have allowed them to emerge as an attractive alternative to surgery in select patient population. These techniques are highly dependent on multimodality imaging for periprocedural planning as well as during the procedure. Computed tomography (CT) allows comprehensive assessment of cardiac/extracardiac structures

This article is part of the Topical Collection on *Cardiac Computed Tomography*

S. V. Gurudevan (✉)
Healthcare Partners Medical Group, Los Angeles, CA 90048, USA
e-mail: sgurudevan@healthcarepartners.com

R. Arsanjani
Cedars-Sinai Heart Institute, Los Angeles, CA, USA

based on its good spatiotemporal resolution. In this review, the role of CT, as it pertains to left atrial appendage occlusion and mitral valve transcatheter procedures, is described.

Left Atrial Appendage Anatomy, Physiology, and Pathology

The left atrial appendage (LAA) is the remnant of the original embryonic left atrium that develops during the 3rd week of gestation. In the adult, it is comprised of 2 major components: the mouth and the body (Fig. 1). The mouth is comprised of the elliptically-shaped LAA orifice and tubular neck, while the body is comprised of 1 or more lobes lined by pectinate muscles [1]. The largest diameter of the elliptical orifice varies in adults from 10 to 40 mm. In a study that examined 500 postmortem human hearts, the authors found that more than 80 % of individuals have multi-lobed LAA bodies [2], where a lobe was defined as the following: (1) it was a visible outpouching from the main tubular body of the LAA, usually demarcated by an external crease; (2) it was internally capable of admitting a 2-mm probe (ie, it was not simply a tag of external adipose tissue); (3) it was occasionally but not necessarily associated with a change in direction of the main tubular body of the LAA; (4) it could lie in a different anatomic plane than the main tubular body; and (5) by definition, the LAA must have at least 1 lobe (ie, a tubular body with a blind-ending sac).

There is emerging data that the LAA has physiologic functions as an endocrine organ as well. It secretes atrial natriuretic peptide as well as B-type natriuretic peptide, especially in patients with atrial fibrillation [3, 4]. Animal studies also suggest that the LAA has stretch receptors that may play a role in the regulation of thirst [5].

The LAA has been implicated as the primary source of thromboembolic stroke in patients with nonvalvular atrial fibrillation [6]. The likelihood of thromboembolic stroke in

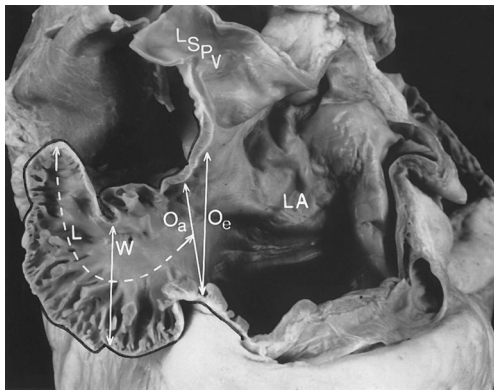


Fig. 1 Gross anatomic view of the left atrium and left atrial appendage (outlined in black). The juxtaposition of the left atrial appendage with the left superior pulmonary vein (LSPV) can also be appreciated. Reproduced with permission from Veinot et al [2]

such patients is related to their risk factors for stroke, which are summarized by the CHADS₂-Vasc scoring system [7, 8]. In this system, patients are assigned 1 point each if they have hypertension, diabetes, congestive heart failure, a history of vascular disease (peripheral arterial disease, coronary artery disease, or cerebrovascular disease), or are greater than 70 years of age, and 2 points if they had a prior stroke or TIA. Patients with CHADS₂-Vasc scores of 2 or more should be treated with anticoagulation to lower the risk of thromboembolism. The magnitude of benefit of an anticoagulation strategy increases as the CHADS₂-Vasc score increases.

Left Atrial Appendage Exclusion Devices in Clinical Practice

In patients with nonvalvular atrial fibrillation who cannot take anticoagulation therapy, exclusion, or occlusion of the left atrial appendage has emerged as novel therapeutic option to reduce the risk of future thromboembolism. There are 2 strategies to accomplish this task. One, termed LAA occlusion, refers to the placement of an intravascular device into the left atrial appendage percutaneously, through a venous access and trans-septal puncture. The 2 most commonly used devices for LAA occlusion are the Watchman Device (Boston Scientific, Natick, MA) (Fig. 2) and the Amplatzer Cardiac Plug (St. Jude Medical, St. Paul, MN) (Fig. 3). Both devices are currently in clinical trials and have not yet received Food and Drug Administration (FDA) approval.

Another therapeutic option is to exclude the LAA from circulation by applying an external ligature—this procedure is termed LAA exclusion. LAA exclusion can be performed surgically using video assisted thoracoscopic surgery (VATS) or percutaneously using the LARIAT device (Sentre Heart, Redwood City, CA)—Fig. 4. Use of the LARIAT device involves the deployment of a magnet into the left atrial appendage employing venous access and trans-septal

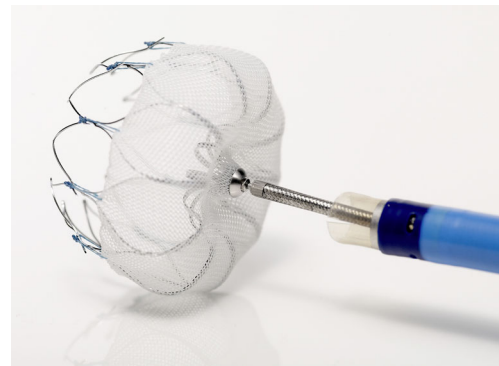


Fig. 2 The Watchman LAA occlusion device (Boston Scientific). The top of the device is covered by expanded polytetrafluoroethylene (ePTFE). The device has nitinol bars that anchor the edges of the device into the LAA. The device is usually oversized by 10 %–20 % of the orifice size of the LAA to allow compression of the device by the LAA tissue after deployment

puncture. Dry pericardial access is also obtained, and a second magnet is introduced through the pericardial space and mates with the first magnet, creating a rail over which a ligation suture can be deployed. The LARIAT device is the only percutaneous LAA exclusion device with FDA approval for use in the United States.

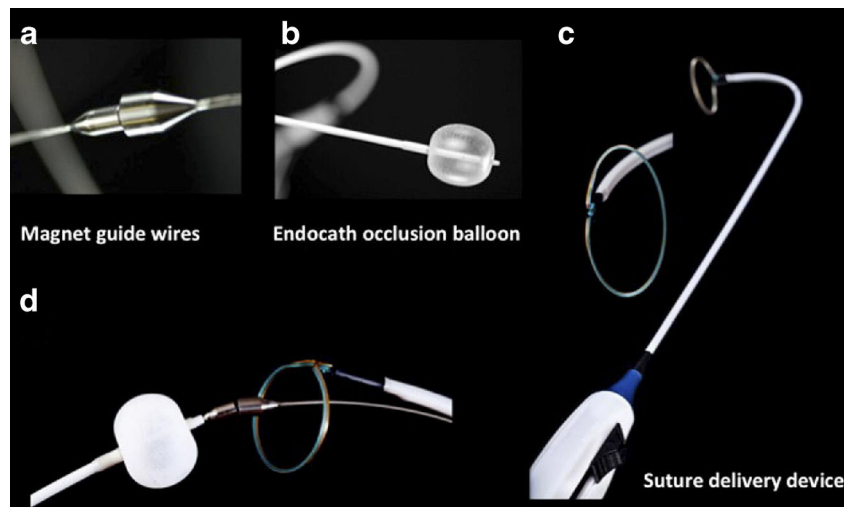
Imaging Considerations Prior to Performance of LAA occlusion

The use of cardiac computed tomography offers the clinician planning a left atrial appendage procedure the opportunity to obtain detailed images of the appendage orifice size, morphology, and course, which are all important parameters to consider when selecting a device of the appropriate size and shape.



Fig. 3 The Amplatzer Cardiac Plug (ACP) LAA occlusion device (St. Jude Medical). The deployment strategy is similar to that involved with the Watchman device. The device is also covered by expanded polytetrafluoroethylene (ePTFE)

Fig. 4 The LARIAT LAA Exclusion System (Sentre Heart). One end of the device is introduced into the left atrial appendage via femoral venous access and trans-septal puncture. The other end of the device is introduced into the pericardial space via dry pericardial access. The 2 ends mate together, creating a rail over which the LARIAT is deployed, effectively ligating the neck of the appendage



It is important to use a consistent imaging protocol to obtain the most diagnostic image quality. Beta-blockers should be administered to the patient to slow the heart rate to below 70 beats per minute. As many patients will be in atrial fibrillation at the time of the study, the images should be reconstructed near end-systole to image the left atrium and LAA during its largest size. Filling of the appendage with contrast can be delayed as a result of atrial fibrillation and delayed imaging can be useful in separating true thrombus from “pseudothrombus” [9, 10]. The principles of good CT imaging of the left atrial appendage are summarized in Table 1.

The left atrial appendage orifice shape is usually elliptical. Cross-sectional measurements of the orifice with calculations of the major and minor axis of the orifice are used to select the appropriately sized device. As a general rule, the device should be oversized by 10 %–20 % of the largest elliptical axis measured as device compression of the same proportion is expected after device deployment. An example of the multiplanar views employed in measuring the left atrial appendage dimension is shown in Fig. 5. Table 2 summarizes the sizing parameters for the Watchman device. Similar strategies are employed when choosing the appropriate size of Amplatzer Cardiac plug for a particular patient.

In a manuscript by Wang et al 4 distinct morphologies of the left atrial appendage were described [11••]. These

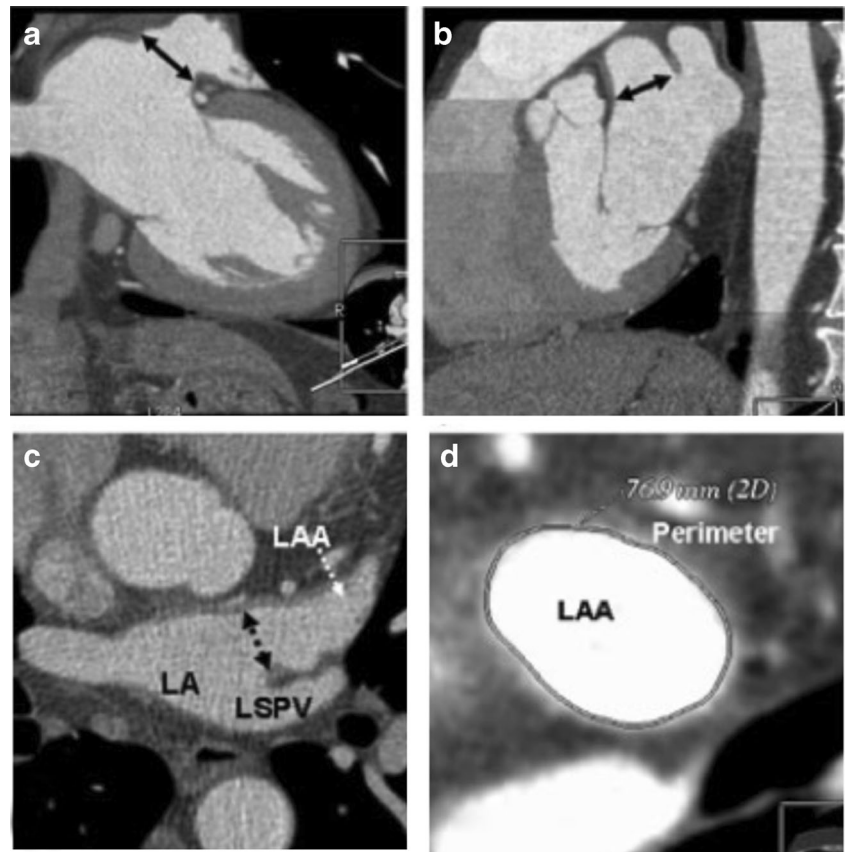
distinct morphologies can influence device selection and can impact procedural success during the left atrial appendage occlusion procedure. The 4 variants include: (1) the chicken-wing morphology (Fig. 6), whose main characteristic is a prominent bend in the proximal or middle part of the dominant lobe or folding back of the LAA anatomy on its self at some distance from the LAA ostium; (2) the windsock morphology, in which there is only the dominant lobe of sufficient length that is the primary structure of the LAA; (3) the cauliflower morphology, whose main characteristic is an LAA that has limited overall length with more complex internal characteristics; and (4) the cactus morphology, whose main characteristic is a dominant central lobe with secondary lobes extending from the central lobe in both superior and inferior directions. Particular appendage morphologies may be associated with a higher risk of thromboembolism. Figure 7 summarizes the 4 different morphologies of LAA that may be encountered.

The type of LAA morphology that the clinician encounters when performing a cardiac CT examination can influence the choice of LAA occlusion device (Watchman vs Amplatzer Cardiac Plug) or the strategy of exclusion or occlusion, as certain morphologies (“chicken wing”) are not favorable for LAA occlusion device deployment. In addition, there is emerging data that suggests that the “chicken wing” LAA morphology may be associated with an increased risk of thromboembolism [12, 13•]. Another important anatomic factor that can be determined with cardiac CT imaging is the course of the LAA. In some patients, the LAA courses behind the pulmonary artery, rendering it inaccessible to a catheter-based ligature from the pericardial approach. These patients are therefore, not candidates for percutaneous exclusion of the LAA with the LARIAT device and should instead have LAA occlusion performed.

Table 1 Keys to good CT imaging of the left atrium and left atrial appendage

Beta-blockade to HR <70
End-systolic reconstruction of dataset
Retrospective gating with ECG-editing of artifacts
Delayed imaging 30 seconds after first-pass CT to separate thrombus from “pseudothrombus”

Fig. 5 The left atrial appendage orifice can be measured in multiple views. Commonly, 2D oblique projections of the appendage, shown in panel **A** and **B**, can demonstrate the long axis dimension of the left atrial appendage, or the major axis of the elliptical LAA orifice. Panel **C** shows a measurement of the LAA near the short axis view of the base of the heart. Measurement in this view gives us the minor axis of the LAA orifice. Panel **D** shows us an “en face” view of the left atrial appendage orifice and reveals its elliptical shape. Both major and minor axis measurements can be obtained in this view



Mitral Valve Percutaneous Procedures Introduction

The incidence of degenerative valvular heart disease continues to increase in the developed countries because of the aging Western population. Aortic stenosis is the most common valvular heart disease in developed countries, while mitral regurgitation affects 7 % of patients ≥ 75 years of age [14]. Surgical intervention has historically represented the primary intervention to alter the disease course in patients with severe aortic stenosis and mitral regurgitation [15]. Recent advances in structural intervention procedures have allowed the increased use of minimally invasive transcatheter interventions, especially in high-risk patients [16, 17••]. The success of these transcatheter based techniques are often dependent on imaging

modalities, including transesophageal echocardiogram and computed tomography (CT), which allow precise visualization of intracardiac structures. These imaging techniques play an important role during patient screening, the procedure, and during the follow-up period in

Table 2 Sizing guidelines for the Watchman device based on LAA maximal diameter

Maximum LAA ostium (mm)	Device diameter (mm)	Device length (mm)
17–19.9	21	20.2
20–22.9	24	22.9
23–25.9	27	26.5
26–28.9	30	29.4
29–31.9	33	31.6

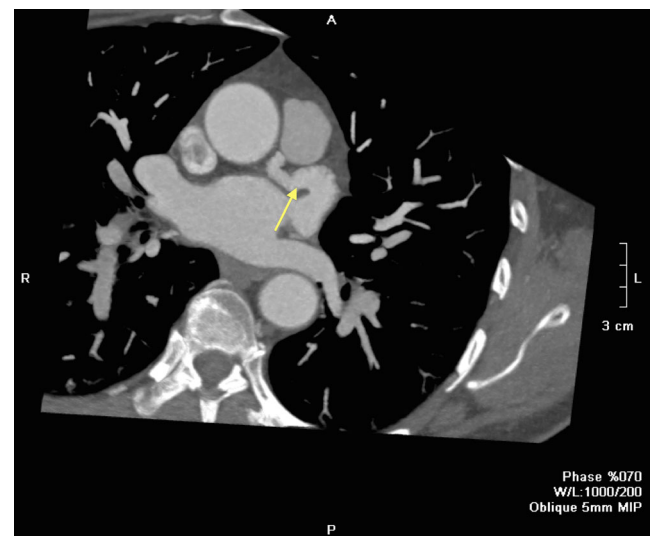
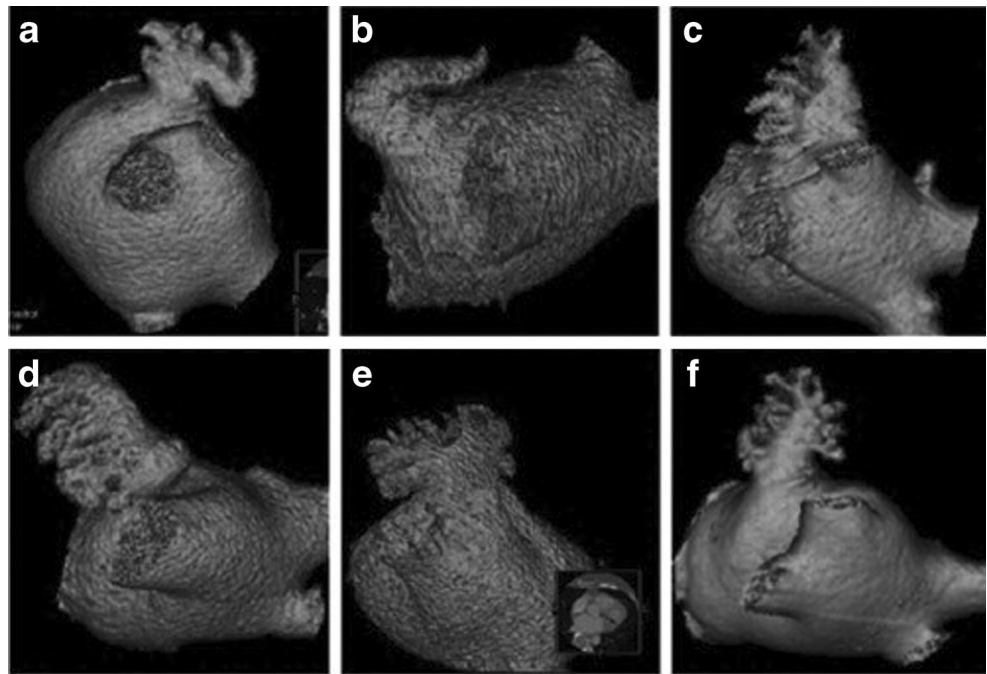


Fig. 6 Axial oblique MIP MDCT projection of the left atrium and LAA. This particular patient has a chicken wing LAA morphology, with a distinct bend in the center of the appendage seen (arrow). When the LAA has a chicken wing morphology, interventional procedures are more challenging and there may be a higher risk of thromboembolism

Fig. 7 3D volume rendered MDCT images demonstrating the 3 different morphologies of left atrial appendage. The chicken wing morphology (Panels A-B) has a distinct bend in the center of the left atrial appendage. The windsock morphology (Panels C-D) has a single dominant lobe with no secondary lobes. The cactus morphology (Panels E-F) has a single dominant lobe with 1 or more secondary lobes. Reproduced with permission from Wang et al [11••]



order to identify feasibility and successful deployment, as well as identifying complications.

Recent advances in 64-slice CT technology have led to significant improvement in spatial and temporal resolution [18]. These advances have allowed coronary CT angiography (CCTA) of 64-detector rows or greater to emerge as

an excellent noninvasive modality for evaluation of coronary arteries. Multiple prior studies have compared the diagnostic performance of CCTA with invasive coronary angiography [19, 20], demonstrating excellent sensitivity and negative predictive value. The use of CCTA for preprocedural screening in transcatheter valvular

Fig. 8 MDCT demonstrating left ventricle in long axis (top left) and short axis (top right). The white arrows mark the papillary muscles, while the red arrows highlight the chordae tendineae. The bottom image demonstrates short-axis of mitral valve divided based on Carpentier's classification. The anterior (AC) and posterior (PC) commissures are noted as well

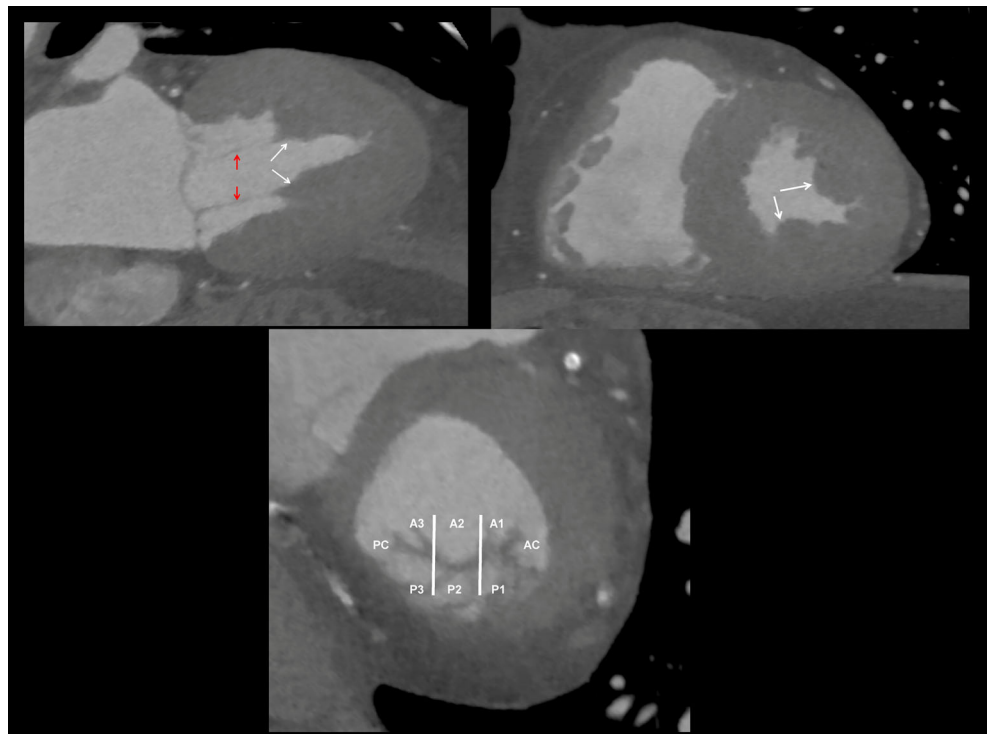


Table 3 Wilkins score for assessment of mitral anatomy

Grade	Mobility	Thickening	Calcification	Subvalvular involvement
1	Highly mobile with only the leaflet tips restricted	Normal thickness (4–5 mm)	A single area of calcification	Minimal thickening just below leaflets
2	Leaflet mid and base portions with normal mobility	Considerable thickening at margins with normal mid-leaflet (5–8 mm)	Scattered areas of calcification confined to leaflet margins	Thickening of 1/3 of chordal structure
3	Valve continues to move forward in diastole (mainly from the base)	Entire leaflet is thickened (5–8 mm)	Calcification extending into mid portion of leaflets	Thickening extending to distal 1/3 of chordal structure
4	No or minimal forward of leaflets movement in diastole	Considerable thickening of all leaflet tissue (>8 mm)	Extensive calcification throughout the leaflet	Extensive thickening of all chords and involves pap muscles

procedures has been steadily increasing. The CCTA is now routinely used for annular sizing and angle of deployment [21–23], however, its use in percutaneous mitral valve procedures has been less well-established. This review focuses on the anatomy of mitral valve apparatus, currently available percutaneous mitral valve procedures, and the use of multi-detector computed tomography (MDCT) as it pertains to percutaneous mitral valve procedures.

Mitral Valve Anatomy and Pathology

The mitral valve apparatus is a complex 3-dimensional structure consisting of the annulus, leaflets, chordae tendineae, and papillary muscles. The annulus is a pliable, oval structure that separates the left atrium and the left ventricle. It exhibits complex motion during the cardiac cycle along with the surrounding ventricular and atrial tissue. The annulus is not a rigid fibrous ring and there is no specific anatomic structure to account for the annulus, but rather it incorporates several structures along its hinge points [24]. The anterior fibrous portion of the annulus is formed by a portion of the left ventricle (membranous septum), the left and right fibrous trigone, as well

as the left and noncoronary sinus of the aortic valve. The other two-thirds of the annulus are mainly muscular, therefore, unlike the fibrous portion of the annulus, more likely to dilate and more prone to calcification [24].

The mitral valve is comprised of 2 leaflets, the anterior and posterior. The anterior leaflet is broader than the posterior leaflet and comprises one-third of the circumference of annulus, however, it is longer from the attachment to the tip. It is arbitrarily divided into 3 regions labeled A1, A2, A3 based on Carpentier's classification (A1 is most lateral adjacent to LAA) [25]. The posterior leaflet on the other hand is narrower and extends two-thirds around the left atrioventricular junction. It often has indentations or 'clefts', which generally form 3 scallops that are also named based on Carpentier's classification (P1 being most lateral) [25].

There are 2 papillary muscles that anchor the leaflets to the left ventricle. The anterolateral papillary muscle is the larger of the 2 and usually has 1 head, while the posteromedial papillary muscle often has multiple heads. There are 3 types of chordae that arise from the papillary muscle tips and insert onto the leaflets in a fan-shaped manner. The primary chords attach to the free edge of the leaflets, while the secondary chords attach to the ventricular surface of the leaflets, and the tertiary chords attach to the basal surface of the posterior leaflet [24]. The

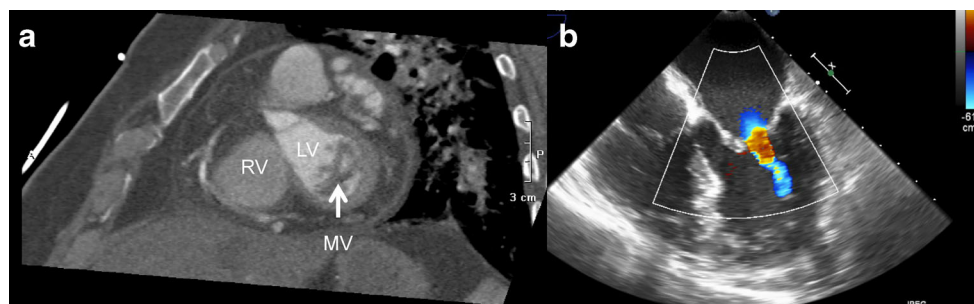


Fig. 9 **A**, MDCT demonstrating significant leaflet thickening and decreased leaflet motion (arrow) in a patient with history of rheumatic mitral stenosis. **B**, Transesophageal echocardiogram demonstrating typical

“hockey-stick” appearance of anterior mitral valve leaflet with flow turbulence into the left ventricle (LV) consistent with mitral stenosis. *LV* left ventricle, *MV* mitral valve, *RV* right ventricle



Fig. 10 Picture of Mitraclip device (Abbott Vascular). The device has an alligator-clip design and is covered by expanded polytetrafluoroethylene (PTFE)

posteromedial papillary muscle supply chords to the medial half of both leaflets, while the anterolateral chords attach to the lateral half of both leaflets (Fig. 8).

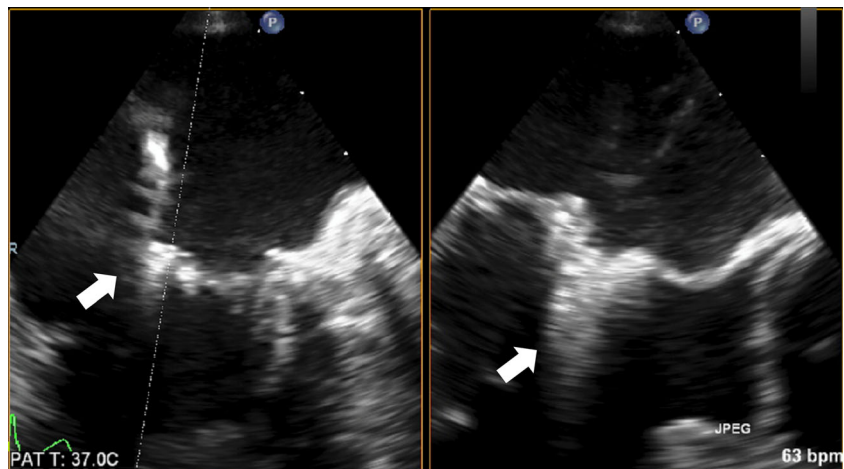
Pathology involving any of the mitral valve apparatus can significantly affect complete coaptation and correct apposition leading to significant mitral regurgitation. Carpentier's functional classification describes leaflet motion as it relates to the annulus [25]. In patients with type 1, there is normal leaflet motion and mitral regurgitation is the result of leaflet perforation (endocarditis) or annular dilation. In those with type 2, there is excessive leaflet motion above the annular plane because of leaflet prolapse or flail, most commonly because of degenerative disease. Finally, type 3 describes significant leaflet restriction and is categorized into 2 groups: 3a, where the leaflets are restricted throughout both systole and diastole (rheumatic heart disease) and 3b, where the restriction is only seen in systole (ischemic mitral regurgitation). Degenerative is most common accounting for more than

one-half of cases, followed by functional ~25 %, and rheumatic ~10 % [24]. Different percutaneous mitral valve procedures have been implemented to address different pathologic processes. These methods along with the role of CT will be further discussed in the following sections.

Percutaneous Mitral Balloon Valvuloplasty for Mitral Stenosis

Percutaneous Mitral Balloon Valvuloplasty (PMBV) is a safe, effective, and less invasive approach compared with surgery for treatment of patients with symptomatic rheumatic mitral stenosis. In appropriately selected patient population, PMBV provides immediate and excellent results comparable to surgical procedures [26]. The most commonly used transthoracic echocardiogram criterion for selecting patients for PMBV is the Wilkins' score [27]. This "splitability score" takes into account 4 factors including severity and extent of leaflet calcification, leaflet thickening, leaflet mobility, and involvement of subvalvular apparatus, each being graded quantitatively on a 1–4 scale (Table 3). There is an inverse relationship between the score and likelihood of success following PMBV with a score of ≤ 8 associated with the best outcomes. A small single center study by White et al evaluated the role of MDCT derived Wilkins' score for predicting mitral valve area changes following PMBV in 23 patients undergoing the procedure (Fig. 9). They were able to demonstrate that the CT-derived score was more predictive of mitral valve area increase following PMBV than the echo-based score, with increased posterior mitral leaflet mobility, decreased leaflet thickness, and absence of subvalvular involvement being associated with improvement in mitral valve area following the procedure [28].

Fig. 11 Transesophageal echocardiogram demonstrating the MitraClip deployed on the anterior and posterior mitral valve leaflets



Percutaneous Approach to Mitral Valve Therapies

As previously mentioned, pathology involving any portion of the mitral apparatus could lead to or contribute to mitral regurgitation. Historically, surgical interventions have primarily aimed at correcting the culprit lesion that lead to mitral regurgitation including repairing leaflets, annulus, commissures, chordae, papillary muscles, and left ventricle. Current percutaneous techniques have also been developed on the basis of these surgical principles. Although, multiple percutaneous experimental approaches are under development for treatment of mitral regurgitation including leaflet based (edge-to-edge repair), coronary sinus based, left atrium based, left ventricular based, or mitral valve replacements, the 2 most commonly used percutaneous procedures (leaflet based and coronary sinus based) will be discussed here.

Edge-to-Edge Repair

This leaflet repair approach is based on Alfieri edge-to-edge repair approach [29]. The most studied and advanced percutaneous edge-to-edge repair device currently available is the MitraClip (Abbott Park, IL, USA) (Fig. 10). The device is delivered using a 24 F steerable delivery guide catheter via a trans-septal approach and places a V-shaped clip (Fig. 11) on the mitral valve leaflets creating an effective double orifice repair (Fig. 12) [30]. In the EVEREST (Endovascular Valve Edge-to-Edge Repair Study) trial, 107 patients with grade 3–4+ mitral regurgitation were treated with the MitraClip. The rate of major adverse events was 9 %, freedom from clip embolization was 100 %, and 74 % of patients achieved acute procedural success with 64 % being discharged with $\leq 1+$ mitral regurgitation [31••]. This study established the safety and

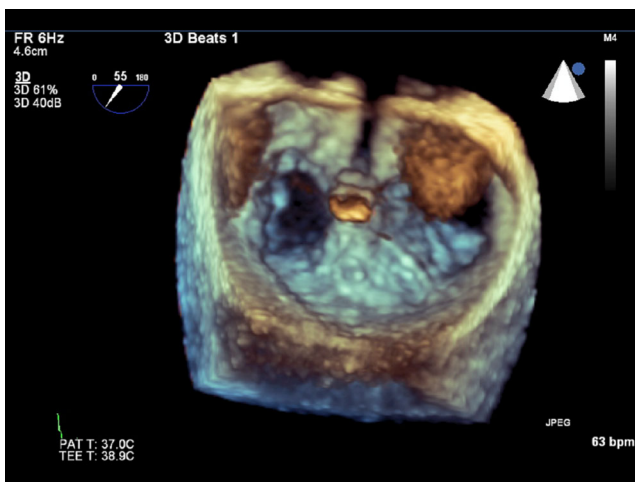


Fig. 12 Three-dimensional transesophageal echocardiogram demonstrating “double orifice” mitral valve following MitraClip deployment

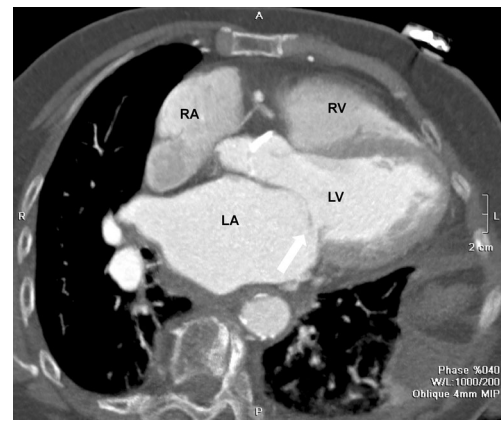


Fig. 13 MDCT demonstrating flail anterior mitral valve leaflet (arrow). LA left atrium, LV left ventricle, RA right atrium, RV right ventricle

feasibility of the device. EVEREST II evaluated the safety and efficacy of MitraClip in patients with significant mitral regurgitation at high risk of surgical mortality rate and showed improvement in mitral regurgitation in the majority of patients as well as improvement in clinical symptoms [16]. MitraClip was recently approved by the FDA.

There are several key anatomic criteria used in patient selection for MitraClip implantation, which should be assessed prior to the procedure. In individuals with functional mitral regurgitation, the length of mitral leaflet coaptation needs to ≥ 2 mm and the depth of mitral leaflet coaptation needs to be ≤ 11 mm. In patients with mitral valve prolapse/flail, the flail gap should be < 10 mm and the flail width should be less than 15 mm. Although mitral leaflets are able to be visualized easily using cine MDCT (Fig. 13), because of limited temporal resolution of CT transesophageal echocardiogram is superior in identifying the mechanism mitral regurgitation and anatomic details of leaflet motion. However, MDCT can provide valuable anatomic information about annular size and extent of calcification, with severe mitral annulus



Fig. 14 MDCT demonstrating severe mitral annulus calcification (arrows). AO aorta, RA right atrium

Fig. 15 The 4-chamber (top left) and 2-chamber (top right) views reconstructed at the level of the mitral annulus. The bottom image demonstrates the short-axis view of mitral annulus with the arrows highlighting the intercommissural and anteroposterior diameters of the mitral annulus

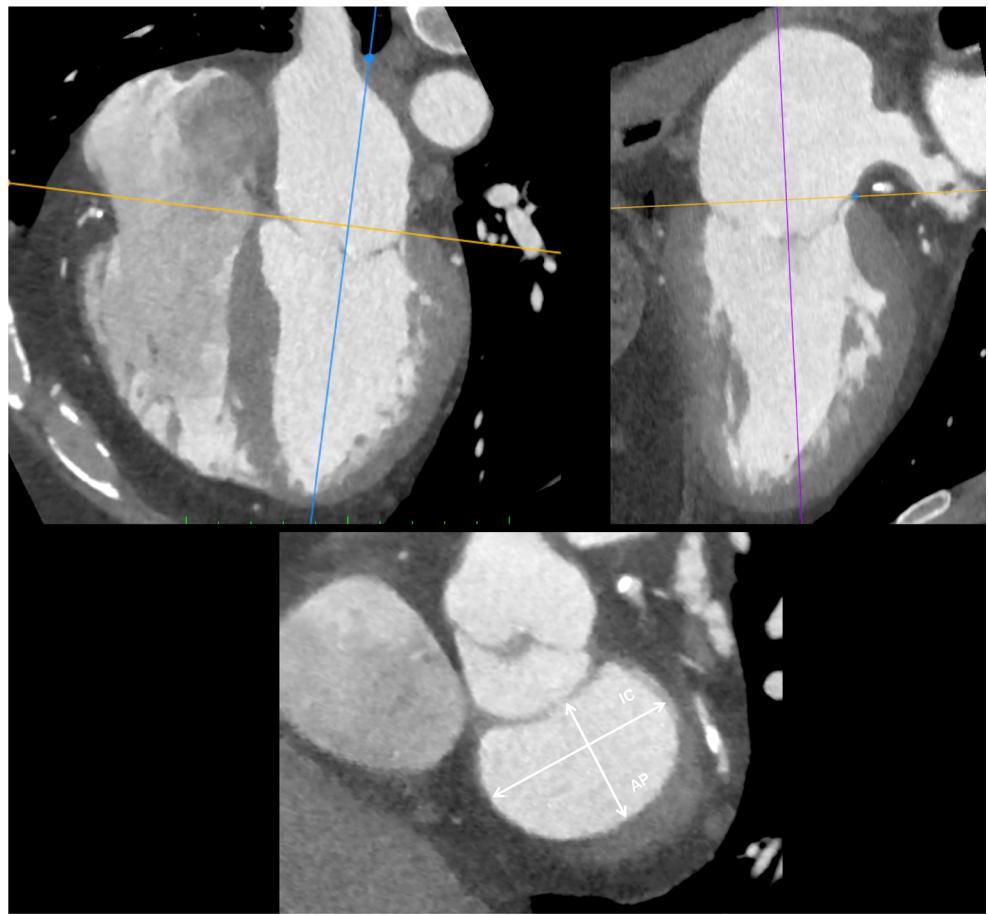


Fig. 16 MDCT demonstrating leaflet tethering and coaptation failure in patient with functional mitral regurgitation. Mitral valve leaflet divided based on Carpentier's classification. *AO* aorta, *LA* left atrium, *LV* left ventricle, *RA* right atrium, *RV*, right ventricle

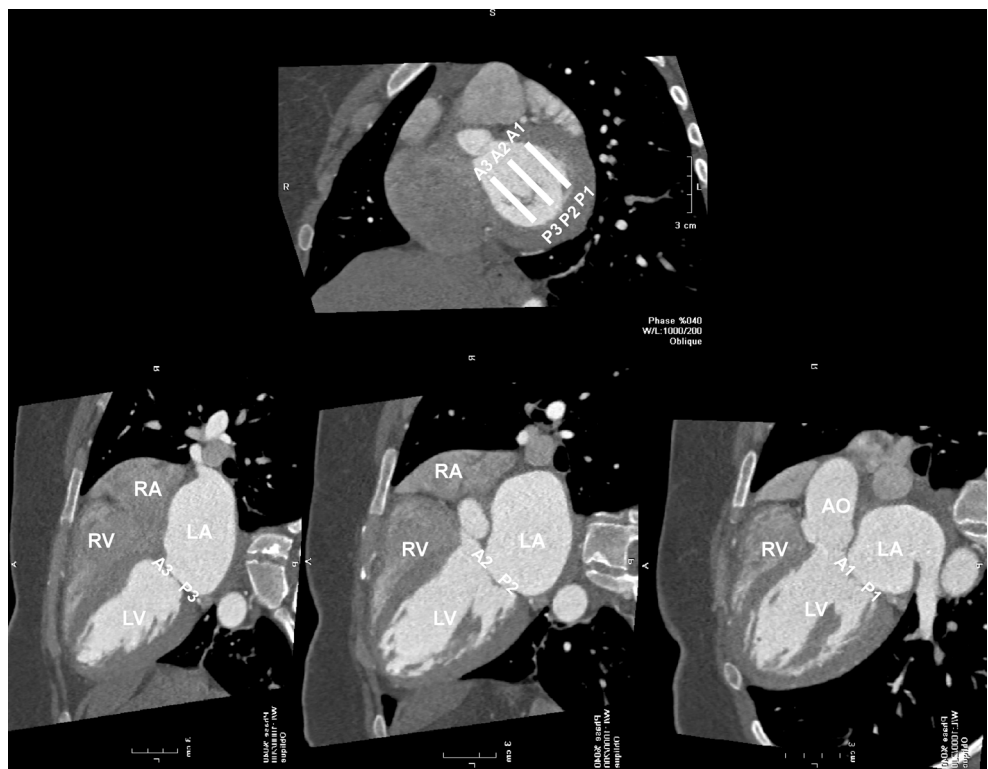




Fig. 17 Picture of Carillon XE

calcification being a potential contraindication to MitraClip implantation (Fig. 14). Furthermore, annular size measurements are easier with CT because of ability to construct the mitral annular plane from the 3-dimensional database (Fig. 15). In addition, MDCT can accurately assess the restriction and tethering of the mitral apparatus, which may be critical in determining the mechanism of mitral regurgitation in patients with functional mitral regurgitation (Fig. 16).

Percutaneous Mitral Annuloplasty

These procedures are primarily performed by implanting the device into the coronary sinus, which can reduce mitral annular dimensions leading to improvement in leaflet coaptation and reduction in mitral regurgitation. The CARILLON Mitral Contour System (Cardiac Dimensions, Washington, USA) is a nitinol-based proximal and distal anchor system connected by a curved nitinol bridge (Fig. 17). The efficacy of this device was evaluated in the AMADEUS (the CARILLON Mitral Annuloplasty Device European Union Study) trial, which was a prospective, multicenter study enrolling 48 patients with dilated cardiomyopathy, moderate to severe FMR, an ejection fraction <40 %, and a 6-minute walk distance between 150 and 450 meters [32]. Eighteen out of 48 patients did not receive the device because of access issues, insufficient acute functional mitral regurgitation reduction, or coronary artery

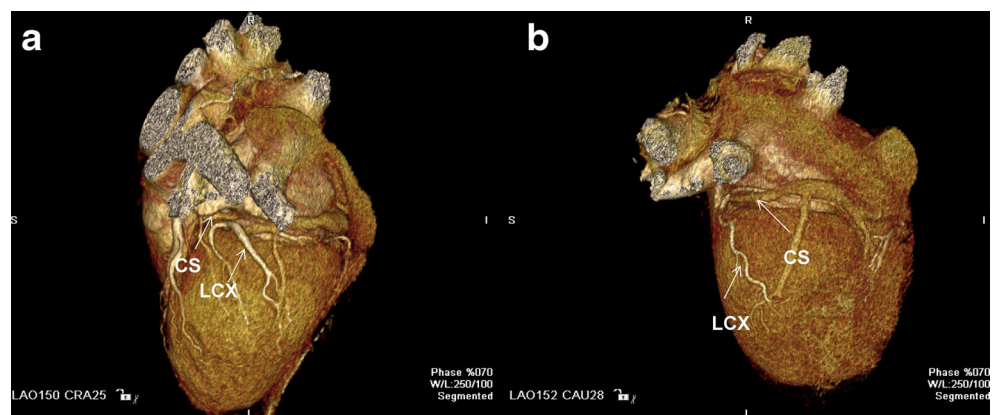
compromise, while major adverse event rate occurred in 13 % of patients at 30 days. At 6-months follow-up, the degree of functional mitral regurgitation based on quantitative echocardiographic measures ranged from 22 % to 32 %, while both 6-minute walk distance and quality of life parameters significantly improved. The CARILLON is not currently FDA approved.

MDCT can provide significant and valuable information about the anatomy of the mitral valve leaflets in patients with degenerative mitral regurgitation [33•]. In addition, it can provide the clinician robust information about the anatomy of the coronary sinus, including the distance to the mitral annulus and the angle between the coronary sinus and mitral annulus. If the angle is too wide, the force applied to the coronary sinus would not be transmitted to the mitral annulus and results will likely be suboptimal. Furthermore, the relationship between the coronary sinus and the left circumflex artery can be elucidated using MDCT. A study by Tops et al demonstrated that in 68 % of patients the left circumflex artery courses between the coronary sinus and the mitral annulus, which could significantly limit the use of percutaneous mitral annuloplasty devices based on concerns about coronary artery compromise (Fig. 18) [34].

Conclusions

In patients who are scheduled to undergo a transcatheter procedure, a preprocedural multimodality imaging approach is likely required. MDCT provides accurate information about left atrial appendage dimensions and presence of thrombus and should be routinely used in patients who are scheduled to undergo left atrial appendage closure. In addition, it provides important information about surrounding structures. In patients undergoing percutaneous mitral valve repair, MDCT provides important information about valvular dimensions and spatial relationship between the mitral valve and surrounding structures including the coronary arteries. This is

Fig. 18 MDCT volume rendered image demonstrating the relationship between the coronary sinus and left circumflex artery. (A) Left circumflex under the coronary sinus; (B) left circumflex over the coronary sinus. CS coronary sinus, LCX left circumflex artery



especially important in patients undergoing percutaneous mitral valve annuloplasty.

Compliance with Ethics Guidelines

Conflict of Interest Swaminatha V. Gurudevan and Reza Arsanjan declare that they have no conflict of interest.

Human and Animal Rights and Informed Consent This article does not contain any studies with human or animal subjects performed by any of the authors.

References

Papers of particular interest, published recently, have been highlighted as:

- Of importance
- Of major importance

- 1.• Alli O, Holmes Jr DR. Left atrial appendage occlusion for stroke prevention. *Curr Probl Cardiol.* 2012;37:405–41. *A comprehensive review of left atrial appendage occlusion by a highly experienced operator.*
2. Veinot JP, Harrity PJ, Gentile F, et al. Anatomy of the normal left atrial appendage: a quantitative study of age-related changes in 500 autopsy hearts: implications for echocardiographic examination. *Circulation.* 1997;96:3112–5.
3. Rodeheffer RJ, Naruse M, Atkinson JB, et al. Molecular forms of atrial natriuretic factor in normal and failing human myocardium. *Circulation.* 1993;88:364–71.
4. Inoue S, Murakami Y, Sano K, et al. Atrium as a source of brain natriuretic polypeptide in patients with atrial fibrillation. *J Card Fail.* 2000;6:92–6.
5. Zimmerman MB, Blaine EH, Stricker EM. Water intake in hypovolemic sheep: effects of crushing the left atrial appendage. *Science.* 1981;211:489–91.
6. Blackshear JL, Odell JA. Appendage obliteration to reduce stroke in cardiac surgical patients with atrial fibrillation. *Ann Thorac Surg.* 1996;61:755–9.
- 7.• Lip GYH, Frison L, Halperin JL, et al. Identifying patients at high risk for stroke despite anticoagulation: a comparison of contemporary stroke risk stratification schemes in an anticoagulated atrial fibrillation cohort. *Stroke J Cereb Circ.* 2010;41:2731–8. *A comparison of the CHADS2-Vasc scoring system to the CHADS2 system is performed in this study, which establishes an incrementally improved ability of the CHADS2-Vasc system to predict thromboembolism in at-risk patients with atrial fibrillation.*
8. Lip GYH, Nieuwlaat R, Pisters R, et al. Refining clinical risk stratification for predicting stroke and thromboembolism in atrial fibrillation using a novel risk factor-based approach: the Euro Heart Survey on atrial fibrillation. *Chest.* 2010;137:263–72.
9. Saremi F, Channual S, Gurudevan SV, et al. Prevalence of left atrial appendage pseudothrombus filling defects in patients with atrial fibrillation undergoing coronary computed tomography angiography. *J Cardiovasc Comput Tomogr.* 2008;2:164–71.
10. Hur J, Kim YJ, Lee H-J, et al. Left atrial appendage thrombi in stroke patients: detection with two-phase cardiac CT angiography versus transesophageal echocardiography. *Radiology.* 2009;251:683–90.
- 11.•• Wang Y, Di Biase L, Horton RP, et al. Left atrial appendage studied by computed tomography to help planning for appendage closure device placement. *J Cardiovasc Electrophysiol.* 2010;21:973–82. *This is the first manuscript that describes the 4 major morphologic appearances of the human left atrial appendage as assessed by cardiac computed tomography.*
12. Kosiuk J, Nedios S, Kornej J, et al (2014) Impact of left atrial appendage morphology on peri-interventional thromboembolic risk during catheter ablation of atrial fibrillation. *Heart Rhythm.*
- 13.• Khurram IM, Dewire J, Mager M, et al. Relationship between left atrial appendage morphology and stroke in patients with atrial fibrillation. *Heart Rhythm.* 2013;10:1843–9. *This manuscript is the first to examine the relationship between left atrial appendage morphology and the risk of thromboembolism, and implicates the “chicken wing” morphology as being associated with a higher risk of thromboembolism in the cohort studied.*
14. Nkomo VT, Gardin JM, Skelton TN, et al. Burden of valvular heart diseases: a population-based study. *Lancet.* 2006;368:1005–11.
15. Nishimura RA, Otto CM, Bonow RO, et al (2014) AHA/ACC guideline for the management of patients with valvular heart disease: executive summary: a report of the American College of Cardiology/American Heart Association Task Force on Practice Guidelines. *J Am Coll Cardiol.*
16. Whitlow PL, Feldman T, Pedersen WR, et al. Acute and 12-month results with catheter-based mitral valve leaflet repair: the EVEREST II (Endovascular valve edge-to-edge repair) high risk study. *J Am Coll Cardiol.* 2012;59:130–9.
- 17.•• Makkar RR, Fontana GP, Jilaihawi H, et al. Transcatheter aortic-valve replacement for inoperable severe aortic stenosis. *N Engl J Med.* 2012;366:1696–704. *Landmark clinical trial, which established transcatheter aortic valve replacement (TAVR) as a viable treatment option for patients with symptomatic severe aortic stenosis who are inoperable.*
18. Flohr TG, Raupach R, Bruder H. Cardiac CT: how much can temporal resolution, spatial resolution, and volume coverage be improved? *J Cardiovasc Comput Tomogr.* 2009;3:143–52.
19. Meijboom WB, Meijs MFL, Schuijf JD, et al. Diagnostic accuracy of 64-slice computed tomography coronary angiography: a prospective, multicenter, multivendor study. *J Am Coll Cardiol.* 2008;52:2135–44.
20. Budoff MJ, Dowe D, Jollis JG, et al. Diagnostic performance of 64-multidetector row coronary computed tomographic angiography for evaluation of coronary artery stenosis in individuals without known coronary artery disease: results from the prospective multicenter ACCURACY (Assessment by Coronary Computed Tomographic Angiography of Individuals Undergoing Invasive Coronary Angiography) trial. *J Am Coll Cardiol.* 2008;52:1724–32.
21. Jilaihawi H, Kashif M, Fontana G, et al. Cross-sectional computed tomographic assessment improves accuracy of aortic annular sizing for transcatheter aortic valve replacement and reduces the incidence of paravalvular aortic regurgitation. *J Am Coll Cardiol.* 2012;59:1275–86.
22. Gurvitch R, Wood DA, Leipsic J, et al. Multi-slice computed tomography for prediction of optimal angiographic deployment projections during transcatheter aortic valve implantation. *JACC Cardiovasc Interv.* 2010;3:1157–65.
23. Leipsic J, Gurvitch R, Labounty TM, et al. Multidetector computed tomography in transcatheter aortic valve implantation. *JACC Cardiovasc Imaging.* 2011;4:416–29.
24. McCarthy KP, Ring L, Rana BS. Anatomy of the mitral valve: understanding the mitral valve complex in mitral regurgitation. *Eur J Echocardiogr.* 2010;11:i3–9.
25. Carpentier AF, Lessana A, Relland JY, et al. The “physio-ring”: an advanced concept in mitral valve annuloplasty. *Ann Thorac Surg.* 1995;60:1177–85. *discussion 1185–6.*

26. Ben Farhat M, Ayari M, Maatouk F, et al. Percutaneous balloon versus surgical closed and open mitral commissurotomy: seven-year follow-up results of a randomized trial. *Circulation*. 1998;97:245–50.
27. Wilkins GT, Weyman AE, Abascal VM, et al. Percutaneous balloon dilatation of the mitral valve: an analysis of echocardiographic variables related to outcome and the mechanism of dilatation. *Br Heart J*. 1988;60:299–308.
28. White ML, Grover-McKay M, Weiss RM, et al. Prediction of change in mitral valve area after mitral balloon commissurotomy using cine computed tomography. *Invest Radiol*. 1994;29:827–33.
29. Alfieri O, Elefteriades JA, Chapolini RJ, et al. Novel suture device for beating-heart mitral leaflet approximation. *Ann Thorac Surg*. 2002;74:1488–93.
30. St Goar FG, Fann JI, Komtebedde J, et al. Endovascular edge-to-edge mitral valve repair: short-term results in a porcine model. *Circulation*. 2003;108:1990–3.
31. •• Feldman T, Kar S, Rinaldi M, et al. Percutaneous mitral repair with the MitraClip system: safety and midterm durability in the initial EVEREST (Endovascular Valve Edge-to-Edge Repair Study) cohort. *J Am Coll Cardiol*. 2009;54:686–94. *Important clinical trial that established the efficacy and safety of percutaneous mitral valve repair using the MitraClip device for edge-to-edge endovascular repair of the mitral valve in patients with symptomatic severe mitral regurgitation.*
32. Schofer J, Siminiak T, Haude M, et al. Percutaneous mitral annuloplasty for functional mitral regurgitation: results of the CARILLON Mitral Annuloplasty Device European Union Study. *Circulation*. 2009;120:326–33.
33. • Smith T, Gurudevan S, Cheng V, et al. Assessment of the morphological features of degenerative mitral valve disease using 64-slice multi detector computed tomography. *J Cardiovasc Comput Tomogr*. 2012;6:415–21. *This manuscript establishes the efficacy of 64-slice cardiac computed tomography in determining the culprit mitral scallop in patients with degenerative mitral regurgitation undergoing cardiac surgery. Cardiac CT was compared with transesophageal echocardiography, with the gold standard being direct examination of the valve at the time of surgery.*
34. Tops LF, Wood DA, Delgado V, et al. Noninvasive evaluation of the aortic root with multi-slice computed tomography implications for transcatheter aortic valve replacement. *JACC Cardiovasc Imaging*. 2008;1:321–30.